Atmos. Meas. Tech. Discuss., 8, 7781–7803, 2015
www.atmos-meas-tech-discuss.net/8/7781/2015/
doi:10.5194/amtd-8-7781-2015

Atmospheric Measurement Techniques Discussions
Open Access

Ionospheric correction of GPS radio occultation data in the troposphere

Z. Zeng, S. Sokolovskiy, W. Schreiner, D. Hunt, J. Lin, and Y.-H. Kuo

COSMIC Project Office, University Corporation for Atmospheric Research, Boulder, Colorado, USA

Received: 19 June 2015 – Accepted: 27 June 2015 – Published: 24 July 2015

Correspondence to: Z. Zeng (zzeng@ucar.edu)

Published by Copernicus Publications on behalf of the European Geosciences Union.

Abstract

For inversions of the GPS radio occultation (RO) data in the neutral atmosphere, this study investigates an optimal transition height for replacing the standard ionospheric correction by the linear combination of the L1 and L2 bending angles with the correction of the L1 bending angle by the L1-L2 bending angle extrapolated from above. The optimal transition height depends on the RO mission (i.e., the receiver and firmware) and is different between rising and setting occultations and between L2P and L2C GPS signals. This height is within the range approximately 10–20 km. One fixed transition height, which can be used for the processing of currently available GPS RO data, can be set to 20 km. Analysis of the L1CA and the L2C bending angles in the presence of a sharp top of the boundary layer reveals differences that can be explained by shifts in the impact parameter. The ionosphere-induced vertical shifts of the bending angle profiles require further investigation.

1 Introduction

When GPS radio occultation (RO) signals are used for monitoring the neutral atmosphere, the ionospheric effect has to be removed. While the neutral atmospheric effect on the RO signals exponentially decreases with the height, the ionospheric effect on the average slowly increases with the height. Thus, removal of the ionospheric effect (i.e. ionospheric correction) is most important in the stratosphere. Nevertheless, neglecting the ionospheric correction in the troposphere results in a small but statistically significant inversion bias. One of the common methods of dual-frequency, model-independent ionospheric correction is a linear combination of the L1 and L2 GPS RO observables and, in particular, the linear combination of the L1 and L2 bending angles taken at the same impact parameter (Vorob'ev and Krasil'nikova, 1994) (hereafter the "standard ionospheric correction"). However, a disadvantage of the standard ionospheric correction is the amplification of uncorrelated noises (errors) on L1 and L2.

AMTD
8, 7781–7803, 2015

When the first GPS RO data became available in 1995 (Ware et al., 1996), it became clear that the standard linear combination of the L1 and L2 bending angles is useless in the troposphere, mainly due to noise and tracking errors in the encrypted L2P signal. In order to approximately remove the mean ionospheric effect, it was proposed that the L1 bending angle be corrected by using the L1-L2 bending angle extrapolated from above the troposphere (Kursinski et al., 1997, 2000; Rocken et al., 1997; Steiner et al., 1999; Hajj et al., 2002). As a result of the open-loop (OL) tracking of the L1 in the troposphere (Sokolovskiy et al., 2009; Ao et al., 2009), the L2P is unavailable and only the ionospheric correction by extrapolation of the L1-L2 can be applied. With the OL tracking of the un-encrypted L2C (Sokolovskiy et al., 2014), both the L1CA and L2C signals, free of the tracking errors, are available in the troposphere. Theoretically, this may allow an extension of the standard ionospheric correction into the troposphere. However, in practice, as noted by several different researchers, not only the noise, but also the small-scale refractivity irregularities in the troposphere may introduce additional errors into the standard ionospheric correction. As it follows from the analysis of the occultations with the L1CA and L2C available in the OL mode (examples shown below in Sect. 1), the standard ionospheric correction down to the surface is feasible for only smooth RO signals under low moisture conditions (e.g., high latitudes, local winter). In the presence of moisture, especially in the tropics, fluctuations of the RO signals result in an increase of noise after the standard ionospheric correction, and extrapolation of the L1-L2 must be applied.

For an optimal application of the ionospheric correction in the troposphere, it is necessary to define the transition height for replacement of the standard linear combination by extrapolation of the L1-L2. It is also necessary to define the extrapolation function and the height interval in which this function is fitted to the L1-L2 and then used to model the L1-L2 below the transition height. In previous studies, the transition height and the fitting interval were not always defined and simple extrapolation functions (constant and linear) were used primarily. In this study, the extrapolation function, which models the effects of the ionospheric F and E layers, is introduced and a special case

AMTD
8, 7781–7803, 2015

of this function is used for processing and statistical analysis of the GPS RO data. The selection of the transition height is based on the noisiness of the ionosphere-corrected bending angle. A transition too high results in an increase of noise due to the uncorrected, small-scale ionospheric effects. A transition too low results in an increase of noise due to the small-scale tropospheric irregularities and L2P tracking errors. An optimal transition height minimizes the noise at all heights. As it follows from the results of this study, the optimal transition height depends on the latitude and is different for different GPS RO receivers and firmware, for L2P and L2C signals, and for setting and rising occultations.

Section 2 presents examples of the occultations with L1CA and L2C available in the OL mode and with the standard ionospheric correction applied down to the surface. Section 3 introduces a model of the L1-L2 bending angle for extrapolation of the ionospheric correction in the troposphere. Section 4 presents statistical distributions of the dynamic transition heights (as determined individually for each occultation). Section 5 presents the statistical comparison of the GPS RO bending angles to those from the European Center for Medium range Weather Forecasting (ECMWF) analysis for different static transition heights. This allows us to determine optimal static transition heights. Section 6 concludes the study.

2 Examples of the standard ionospheric correction in the troposphere

The effect of uncorrelated L1 and L2 random errors on the ionospheric correction is known. Let α_1 and α_2 be the L1 and L2 bending angles and β_1 and β_2 their observational noises (errors), whereas $f_1 = 1.57542\,\text{GHz}$ and $f_2 = 1.2276\,\text{GHz}$ are the GPS frequencies. The 1st order ionosphere-free bending angle is equal to

$$\alpha = c_1\alpha_1 - c_2\alpha_2, \tag{1}$$

where $c_1 = f_1^2/(f_1^2 - f_2^2) \cong 2.55$ and $c_2 = f_2^2/(f_1^2 - f_2^2) \cong 1.55$.

For the uncorrelated, random errors β_1 and β_2, the root mean square (rms) error of the ionosphere-free bending angle equals

$$\langle\beta^2\rangle^{1/2} = \left(c_1^2\left\langle\beta_1^2\right\rangle + c_2^2\left\langle\beta_2^2\right\rangle\right)^{1/2}. \tag{2}$$

If the uncorrelated L1 and L2 random errors have the same rms magnitudes ($\langle\beta_1^2\rangle = \langle\beta_2^2\rangle$), then, after the ionospheric correction, the rms error is amplified by a factor of $(c_1^2 + c_2^2)^{1/2} \cong 3$.

Figure 1 shows $\alpha_1(h)$, $\alpha_2(h)$, and $\alpha(h)$, where $h = a - r_c$ is the impact height (a is the impact parameter, r_c is the curvature radius) for the Constellation Observation System for Meteorology, Ionosphere, and Climate (COSMIC) occultations with the L1CA and L2C acquired in the OL mode in the troposphere. Bending angles were calculated from the complex RO signals with the use of wave optics (WO) transform (phase matching) (Jensen et al., 2004) and then smoothed with the window of 0.1 km. To explain some effects in Fig. 1, modeling of the RO signals by the ray-tracing and multiple phase screen method (Sokolovskiy, 2001) with the inversion by WO canonical transform (Gorbunov, 2002) was performed.

Figure 1a shows a high-latitude wintertime occultation. Both $\alpha_1(h)$ and $\alpha_2(h)$ are smooth functions due to low humidity resulting in small fluctuations of refractivity. The fluctuation of $\alpha(h)$ is not substantially different from those of $\alpha_1(h)$ and $\alpha_2(h)$. The standard ionospheric correction performs satisfactorily in the troposphere.

Figure 1b shows a tropical occultation affected by strong random refractivity irregularities caused by moist convection in the troposphere, which broaden the spectra of RO signals both in time and impact height representations (Gorbunov et al., 2006; Sokolovskiy et al., 2010). Correspondingly, $\alpha_1(h)$ and $\alpha_2(h)$ have strong fluctuations that are partially uncorrelated. These uncorrelated fluctuations are caused by large errors of the extracted phase (and frequency) of the WO-transformed signals in the regions of small amplitude (Sokolovskiy et al., 2014). After applying the standard ionospheric correction, these fluctuations are amplified. This is seen in Fig. 1b and was

AMTD
8, 7781–7803, 2015

also confirmed by modeling. We note that an amplification of noise occurs after the standard ionospheric correction is applied in the moist convective troposphere without L1 and L2 tracking errors and does not substantially depend on the ionospheric state. This was also confirmed through the use of modeling. Thus, in the moist convective troposphere, the standard ionospheric correction results in a large amount of noise. The correction by extrapolation is required to obtain a substantial noise reduction.

Figure 1c and d shows two occultations affected by strong refractivity gradients on top of the boundary layer, resulting in the large bending angle gradients and lapses around $h \sim 3.4$ km and $h \sim 2.8$ km. The ionospheric electron density profiles (Abel-retrieved from the differential total electron content) also are shown. The errors of the standard ionospheric correction increase slightly around $h \sim 3.5$ km in Fig. 1c and substantially around $h \sim 2.8$ km in Fig. 1d. This error increase can be explained by the fact that $\alpha_1(h)$ and $\alpha_2(h)$ not only include additive ionospheric contributions $\Delta\alpha_1(h)$ and $\Delta\alpha_2(h)$, but are also shifted in the impact height by Δh_1 and Δh_2. We note that in the case of a circular receiver orbit ($r = \text{const}$) and an immovable transmitter (a geometry close to the GPS RO from a low Earth orbit), the impact parameter $a = rn\sin\varphi$ is directly related to the Doppler frequency shift $f_\mathrm{d} = f(v/c)n\sin\varphi$ (where v, n, φ are velocity, refractive index, and the zenith angle of the ray at the receiver separately) and does not depend on the refractive index n at the receiver. Thus, neglecting electron density at the receiver does not introduce an error of a, by only introducing an error of $\alpha_{1,2}$ which, in the 1st order, is eliminated by the standard ionospheric correction. This was confirmed through the use of ray tracing. However, wave optics modeling and the inversion of RO signals result in the shifts $\Delta h_{1,2}$, similar to those seen in Fig. 1d at $h \sim 2.8$ km, which depend mainly on the electron density at the receiving height. We note that electron density at the receiver height (~ 800 km) in Fig. 1d is about 4 times larger than in Fig. 1c (while the maximum F2 electron density is larger by only about 40 %).

Extrapolation of the ionospheric correction (discussed in the next section) eliminates the errors such as those around ~ 2.8 km in Fig. 1d. However, if the ionosphere results

Discussion Paper | Discussion Paper | Discussion Paper | Discussion Paper |

AMTD

8, 7781–7803, 2015

in impact height shifts, this may be important for RO monitoring of the boundary layer depth and, especially, its weak diurnal variations over the oceans (Sokolovskiy et al., 2011; Ho et al., 2015) because of possible aliasing of the strong ionospheric diurnal cycle. Investigation of the possible ionosphere-induced impact height shifts is outside the scope of this study and will be considered in the future.

3 Ionospheric correction by extrapolation of L1-L2 bending angle

The standard ionosphere-corrected bending angle can be written in the form:

$$\alpha(h) = c_1\alpha_1(h) - c_2\alpha_2(h) = \alpha_1(h) + c_2[\alpha_1(h) - \alpha_2(h)]. \quad (3)$$

At heights where errors of $\alpha_2(h)$ become too large (such as in the troposphere), it makes sense to approximate $\alpha_1(h) - \alpha_2(h)$ by a smooth function $\alpha_{ext}(h)$, which is fitted to $\alpha_1(h) - \alpha_2(h)$ at some interval (h_{ext}, h_{top}) where the errors of α_2 are not too large:

$$\int_{h_{ext}}^{h_{top}} [\alpha_1(h) - \alpha_2(h) - \alpha_{ext}(h)]^2 \mathrm{d}h = \min \quad (4)$$

and, at $h < h_{ext}$, to replace Eq. (3) with

$$\alpha(h) = \alpha_1(h) + c_2\alpha_{ext}(h). \quad (5)$$

The ionospheric correction by extrapolation eliminates the errors of α_2 by instead introducing the errors due to uncorrected small-scale ionospheric effects on α_1. If the α_2 errors are larger than the small-scale ionospheric effects, the ionospheric correction by extrapolation results in the overall reduction of the magnitude of bending angle error. Such replacement of the errors may also change the vertical error correlation, as noted by Syndergaard et al. (2013), but investigation of this effect is outside the scope of this study.

AMTD

8, 7781–7803, 2015

Title Page
Abstract Introduction
Conclusions References
Tables Figures
◄ ►
Back Close
Full Screen / Esc
Printer-friendly Version
Interactive Discussion

Since, on average, $\alpha_1 - \alpha_2$ is a smooth function, in previous studies, α_{ext} was either a constant or linear function (Kursinski et al., 1997, 2000; Rocken et al., 1997; Steiner et al., 1999) fitted to the observational $\alpha_1 - \alpha_2$ in some interval above the extrapolation height. However, $\alpha_1 - \alpha_2$ is also affected by the ionospheric irregularities and L2 tracking errors. To reduce these effects on α_{ext}, it makes sense to increase the fitting interval and to apply a more complicated model of the ionospheric effect on bending angle. For this purpose, we first calculate the bending angle response $\delta\alpha$ from an infinitely thin refractivity layer (modeled by delta-function) at a height z_0:

$$\delta\alpha(h) \sim \int_h^\infty \frac{\mathrm{d}\delta(z-z_0)/\mathrm{d}z}{(z-h)^{1/2}}\mathrm{d}z \sim \left.\frac{\delta(z-z_0)}{(z-h)}\right|_h^\infty - \int_h^\infty \frac{\delta(z-z_0)}{(z-h)^{3/2}}\mathrm{d}z \sim (z_0-h)^{-3/2}. \quad (6)$$

The ionospheric layer, such as F2, is not thin. However, Healy and Culverwell (2015) calculated the bending angle response from the Chapman layer and found that at heights lower than the maximum by two height scales the response is well approximated by $(z_0 - h)^{-3/2}$, i.e. is the same as those from the delta function. The same approximation must be valid for a thinner E layer. Thus, we model the ionospheric bending angle by the function:

$$\alpha_{ext}(h) = A + B \cdot h + C(z_E - h)^{-3/2} + D(z_{F2} - h)^{-3/2}, \quad (7)$$

where $z_E = 100$ km and $z_{F2} = 300$ km are approximate heights of the E and F2 layers. We note that only one term, similar to the last one on the right hand of Eq. (7), was considered in the model for extrapolation of $\alpha_1 - \alpha_2$ by Culverwell and Healy (2012). However, our tests show that all terms in conjunction are important (in particular, the first two terms are needed for modeling of the effects of horizontal inhomogeneity of the ionosphere). We search for coefficients A, B, C, and D by the least squares fitting of $\alpha_{ext}(h)$ to the observational $\alpha_1(h) - \alpha_2(h)$ in the interval $h_{ext} < h < 80$ km. Figure 2a shows $\alpha_1(h) - \alpha_2(h)$ and $\alpha_{ext}(h)$ for six COSMIC occultations for $h_{ext} = 20$ km. Figure 2b

AMTD
8, 7781–7803, 2015

Ionospheric correction of GPS radio occultation data in the troposphere

Z. Zeng et al.

shows the same but with an excluded fourth term in Eq. (6). It is seen from a comparison of Fig. 2a and b that keeping the fourth term in $\alpha_{\mathrm{ext}}(h)$ results in an over fitting. Thus, it is sufficient to keep the third term which models the response from the E layer, while the response from the F2 layer, as well as the effects of horizontal inhomogeneity of the ionosphere, are modeled by the first two terms. In the following, the function

$$\alpha_{\mathrm{ext}}(h) = A + B \cdot h + C(z_{\mathrm{E}} - h)^{-3/2} \tag{8}$$

is used for extrapolation of the ionospheric correction.

4 Dynamic transition height for extrapolation of the ionospheric correction

One of the options used in the COSMIC Data Analysis and Archive Center (CDAAC) inversion algorithm, checks the L2 quality from top to bottom based on a simple criterion $|\Delta s_1 - \Delta s_2| < 6$ cm, where Δs_1 and Δs_2 are raw (unsmoothed) excess phase changes between 50 Hz samples (Kuo et al., 2004). The standard ionospheric correction is replaced by extrapolation below the height (called the L2 drop height, same as the transition height), defined as the maximal height below 40 km where this criterion is not satisfied or the height where L2 becomes unavailable. Occultations with an L2 drop height above 20 km are not processed. The most common reason for a large $|\Delta s_1 - \Delta s_2|$ is a strong fluctuation of the RO signal resulting in an L2P tracking instability. The threshold of 6 cm (approximately 1/4 of an L2 wavelength) has no clear physical justification and was found empirically based on the processing of a large amount of RO data and as a tradeoff between the quality (i.e. noisiness) and quantity (i.e. number of processed occultations).

Figure 3 shows the latitudinal distributions of the L2 drop heights for April 2012. Figure 3a and b shows the L2P drop heights for the COSMIC setting and rising occultations. The upper part of the "donut shaped" structure in Fig. 3b is correlated with the height of the tropopause. In many occultations, the sharp structure of the tropopause is sufficient to cause a strong enough fluctuation of the RO signal that it results in a tracking instability of the L2P. For those occultations where the L2P tracking remains sufficiently stable at the tropopause, it becomes unstable in the presence of fluctuations caused by the tropospheric moisture, or the L2 becomes unavailable below the transition height from the phase-locked loop (PLL) to the OL mode; this explains the lower part of the "donut-shaped" structure. For rising COSMIC occultations, the structure of the distribution of the L2P drop heights is, in general, similar to that of the setting occultations, except that the lower part is higher because the OL-PLL transition generally needs extra time for locking on the L2P and this, on average, happens higher than the PLL-OL transition for setting occultations. The L2C drop heights for COSMIC setting occultations (Fig. 3c) are primarily related to the PLL-OL transition; this confirms that the L2C PLL tracking is stable and not susceptible to signal fluctuations (Sokolovskiy et al., 2014). Although there are some differences, the structures of the distributions of the L2P drop heights for the Meteorological Operational satellite programme (METOP) occultations prior to the 2013 firmware update (Fig. 3d and e) are, in general, similar to those for COSMIC. For setting occultations (Fig. 3e), fewer occultations are affected by the L2P tracking instability induced by the tropopause; and, due to the dynamic PLL-OL transition, the L2P can, on average, be more stably tracked down to the lower height in the troposphere than for COSMIC (Fig. 3b). For rising occultations (Fig. 3d), the lock on the L2P happens, on average, at lower heights than for COSMIC (Fig. 3a). Overall, the comparison of Fig. 3a–e suggests less noisy (more stable) L2P tracking for METOP than for COSMIC.

As it follows from Fig. 3, the dynamic approach for extrapolation of the ionospheric correction results in a rather large spread of the L2P drop heights in low latitudes as well as systematic differences of the L2 drop heights for different missions, rising and setting occultations, and L2P and L2C signals. Generally, this approach may be optimal for the processing of RO data for general purposes and weather applications. An alternative (static) approach applies extrapolation of the ionospheric correction below a fixed transition height that is pre-determined based on statistical evaluation and

AMTD
8, 7781–7803, 2015

minimization of the inversion errors. We believe that the static approach, when all occultations are processed in the same way, may be superior for climate applications.

5 Estimation of the optimal fixed transition height for extrapolation of the ionospheric correction

In this section, we investigate the effect of different transition heights for extrapolation of the ionospheric correction on the retrieved ionosphere-free bending angle profiles. For retrieval of the L1 bending angle, the phase matching method (Jensen et al., 2004) is applied up to 20 km or the transition height h_{ext} (whichever is higher), and geometric optics is applied above. For retrieval of the L2 bending angle, the geometric optics is applied. To evaluate the retrieved ionosphere-free bending angle profiles, they are statistically compared to the bending angles obtained from the ECMWF global analyses, by calculating the mean (bias) and standard deviation. A transition too high results in the increase of random errors due to uncorrected, small-scale ionospheric effects, while transition too low results in the increase of random errors due to noise and tracking errors on the L2. Although the ECMWF model, which is used as the reference, also has errors, it is important that both the errors related to uncorrected ionospheric effects and L2 noise are uncorrelated with the model errors. Consequently, the minimal standard deviation (where all independent errors are summed with squares) can be used as the criterion for finding an optimal transition height. The mean deviation (where all biases are summed with their signs), generally, cannot be used as such a criterion unless the bias becomes too large and can be clearly attributed to RO rather than to the model.

Figures 4 through 7 show statistical comparisons of the RO-retrieved ionosphere-free bending angles to the bending angles forward-modeled from the ECMWF analyses for April 2012. Solid and dashed lines show the mean and standard deviations, respectively. Different colors correspond to different transition heights applied for extrapolation of the ionospheric correction. In each case, an optimal transition height is

AMTD
8, 7781–7803, 2015

located between those fixed heights which result in smaller standard deviations at all heights. More accurately, the optimal transition height can be estimated as the height where the difference between these standard deviations for the fixed heights changes the sign. For the optimal transition height, the standard deviation should be the smallest at all heights.

Figure 4 shows the statistics for the COSMIC L2P with transition heights at 25, 20, 15, and 10 km over three latitude bands. It is apparent that if the transition is too high, such as at 25 km, the standard deviation in some interval (~ 5 km) below the transition height increases, which indicates the noise from uncorrected small-scale ionospheric structures. If the transition is too low, such as at 15 or 10 km, the standard deviation in some interval above the transition height (~ 5–10 km) substantially increases. Clearly, involving the noisy L2P in the ionospheric correction significantly deteriorates the statistical results. The optimal transition heights for different latitudes are not very different, ranging from ~ 17 km at high latitudes to ~ 19 km at low latitudes. Figure 5 shows the statistics for the COSMIC L2P rising and setting occultations. Again, the optimal transition heights are not very different: slightly lower for setting (~ 18 km) than for rising (~ 19 km) occultations. This difference may suggest, on average, lower quality of the L2P signal right after lock (for rising occultations), than after tracking for an extended time (as is the case for setting occultations). We also examine the statistics for the METOP L2P rising and setting occultations before the 2013 firmware update in Fig. 6. The optimal transition heights are ~ 15 and ~ 20 km for setting and rising occultations, respectively. A comparison of Figs. 5 and 6 shows that METOP has a smaller standard deviation (i.e. better L2P quality) than COSMIC, especially for setting occultations. Figure 7a shows statistics for the COSMIC L2C setting occultations (rising L2C occultations currently are not available). The optimal transition height is about 10 km. Because the L2C is tracked in the OL mode down to the bottom of the occultations, Fig. 7b also shows the standard deviation in the lower troposphere for a transition height at 10 km and for the standard ionospheric correction without extrapolation. It is apparent that the application of the standard ionospheric correction down to the bottom of the occulta-

AMTD
8, 7781–7803, 2015

tions makes the ionosphere-free bending angles in the lower troposphere, on average, noisier than the correction by extrapolation below 10 km.

6 Conclusions

Application of the standard ionospheric correction for the L1 and L2 GPS RO bending angles results in an increase of random errors in the troposphere due to noise and tracking errors (mainly on the L2P signal) and tropospheric irregularities, and is also limited by availability of the L2 signal. Correction of the L1 bending angle by the L1-L2 bending angle extrapolated from above reduces these errors by introducing other errors due to uncorrected small-scale ionospheric effects. The extrapolation height, which minimizes the combination of both errors, is considered optimal and depends mainly on the quality of the L2 signal, which, in turn, depends on the receiver, tracking firmware, signal strength and structure, and may depend on the tropospheric and ionospheric irregularities.

Results of this study show that the optimal transition height for the COSMIC L2P occultations is about 20 km (the height differs slightly for different latitudes and for rising and setting occultations). For METOP occultations before the 2013 firmware update, the optimal transition height is about 20 km for rising and ~ 15 km for setting occultations, thus indicating a less noisy L2P than for COSMIC.

For the COSMIC L2C setting occultations (tracked in the OL mode in the lower troposphere), the optimal transition height is about 10 km. Extension of the standard ionospheric correction without extrapolation down to the bottom of the occultations increases the noisiness of the ionosphere-free bending angles in the troposphere. Analysis of L1CA and L2C bending angle profiles around the sharp top of the boundary layer reveals large errors of the standard ionospheric correction, which may be the result of different vertical shifts of the L1 and L2 profiles. Investigation of possible ionosphere-induced vertical shifts of the bending angle profiles will be considered in the future.

AMTD
8, 7781–7803, 2015

To minimize the noise of the ionosphere-free bending angles, occultations from different missions, rising and setting occultations, and L2P and L2C occultations can all be processed with different extrapolation heights. Alternatively, an optimal extrapolation height can be determined for each occultation individually. However, when GPS RO data are used for climate applications, different or dynamically determined extrapolation heights may result in different biases, which may propagate into climate signals. Thus, for climate applications, a constant extrapolation height may be superior. Based on the results of this study, for currently available GPS RO data, a transition height of 20 km (when the L2 is available down to that height) may be considered reasonable.

Acknowledgements. This work is supported by the National Science Foundation under Cooperative Agreement No. AGS-1033112. The authors acknowledge the contributions to this work from members of the COSMIC team at UCAR. The authors are grateful to Stig Syndergaard (DMI) for useful discussions.

References

Ao, C. O., Hajj, G. A., Meehan, T. K., Dong, D., Iijima, B. A., Mannucci, J. A., and Kursinski, E. R.: Rising and setting GPS occultations by use of open-loop tracking, J. Geophys. Res., 114, D04101, doi:10.1029/2008JD010483, 2009.

Culverwell, I. and Healy, S.: Ionospheric correction of RO signals by direct modeling of the ionosphere, Presentation at IROWG-2 Workshop, Estes Park, CO, USA, 28 March–03 April, available at: http://irowg.org/wpcms/wp-content/uploads/2013/12/culverwell.pdf (last access: 4 May 2015), 2012.

Gorbunov, M. E.: Canonical transform method for processing radio occultation data in the lower troposphere, Radio Sci., 37, 1076, doi:10.1029/2000RS002592, 2002.

Gorbunov, M. E., Lauritsen, K. B., Rhodin, A., Tomassini, M, and Kornblueh, L.: Radio holographic filtering, error estimation and quality control of radio occultation data, J. Geophys. Res., 111, D10105, doi:10.1029/2005JD006427, 2006.

Hajj, G. A., Krusinski, E. R., Romans, L. J., Bertiger, W. I., and Leroy, S. S.: A technical description of atmospheric sounding by GPS occultation, J. Atmos. Sol.-Terr. Phy., 64, 451–469, doi:10.1016/S1364-6826(01)00114-6, 2002.

AMTD

8, 7781–7803, 2015

Ionospheric correction of GPS radio occultation data in the troposphere

Z. Zeng et al.

Healy, S. B. and Culverwell, I. D.: A modification to the ionospheric correction method used in GPS radio occultation, Atmos. Meas. Tech. Discuss., 8, 1177–1201, doi:10.5194/amtd-8-1177-2015, 2015.
Ho, S.-P., Peng, L., Anthes, R., Kuo, Y.-H., and Lin, H.-C.: Marine boundary layer heights and their longitudinal, diurnal and interseasonal variability in the Southeastern Pacific using COSMIC, CALIOP, and radiosonde data, J. Climate, 28, 2856–2872, doi:10.1175/JCLI-D-14-00238.1, 2015.
Jensen, A. S., Lohmann, M. S., Nielsen, A. S., and Benzon, H.-H.: Geometrical optics phase matching of radio occultation signals, Radio Sci., 39, RS3009, doi:10.1029/2003RS002899, 2004.
Kuo, Y.-H., Wee, T.-K., Sokolovskiy, S., Rocken, C., Schreiner, W., Hunt, D., and Anthes, R. A.: Inversion and error estimation of GPS radio occultation data, J. Meteorol. Soc. Jpn., 82, 507–531, 2004.
Kursinski, E. R., Hajj, G. A., Schofield, J. T., Linfield, R. P., and Hardy, K. R.: Observing Earth's atmosphere with radio occultation measurements using the Global Positioning System, J. Geophys. Res., 102, 23429–23465, doi:10.1029/97JD01569, 1997.
Kursinski, E. R., Hajj, G. A., Leroy, S. S., and Herman, B.: The GPS radio occultation technique, TAO, 11, 53–114, 2000.
Rocken, C., Anthes, R., Mxner, M., Hunt, D., Sokolovskiy, S., Ware, R., Gorbunov, M., Schreiner, W., Feng, D., Herman, B., Kuo, Y.-H., and Zou, X.: Analysis and validation of GPS/MET data in the neutral atmosphere, J. Geophys. Res., 102, 29849–29866, doi:10.1029/97JD02400, 1997.
Sokolovskiy, S. V.: Modeling and inverting radio occultation signals in the moist troposphere, Radio Sci., 36, 441–458, doi:10.1029/1999RS002273, 2001.
Sokolovskiy, S., Rocken, C., Schreiner, W., Hunt, D., and Johnson, J.: Postprocessing of L1 GPS radio occultation signals recorded in open-loop mode, Radio Sci., 44, RS2002, doi:10.1029/2008RS003907, 2009.
Sokolovskiy, S., Rocken, C., Schreiner, W., and Hunt, D.: On the uncertainty of radio occultation inversions in the lower troposphere, J. Geophys. Res., 115, D22111, doi:10.1029/2010JD014058, 2010.
Sokolovskiy, S., Lenschow, D. H., Zeng, Z., Rocken, C., Schreiner, W. S., Hunt, D. C., Kuo, Y.-H., and Anthes, R. A.: Monitoring the depth of the atmospheric boundary layer by FORMOSAT-3/COSMIC, Presentation at 5th FORMOSAT-3/COSMIC Data Users Workshop, Taipei, Tai-

wan, available at: http://nldr.library.ucar.edu/repository/collections/OSGC-000-000-004-454 (last access: 8 May 2015), 2011.
Sokolovskiy, S. V., Schreiner, W. S., Zeng, Z., Hunt, D. C., Kuo, Y.-H., Meehan, T. K., Stecheson, T. W., Mannucci, A. J., and Ao, C. O.: Use of the L2C signal for inversions of GPS radio occultation data in the neutral atmosphere, GPS Solut., 18, 405–416, doi:10.1007/s10291-013-0340-x, 2014.
Steiner, A. K., Kirchengast, G., and Ladreiter, H. P.: Inversion, error analysis, and validation of GPS/MET occultation data, Ann. Geophys., 17, 122–138, doi:10.1007/s00585-999-0122-5, 1999.
Syndergaard, S., Lauritsen, K. B., Wilhelmsen, H., and Larsen, K. R.: Analysis of Metop/GRAS data products with new on-board tracking parameters and L2 extrapolation, Presentation at Joint OPAC-5/IROWG-3 Workshop, Leibnitz, Austria, 05–11 September, available at: http://www.uni-graz.at/opacirowg2013/data/public/files/opac2013_Stig_Syndergaard_presentation_730.pdf (last access: 26 May 2015), 2013.
Vorob'ev, V. V. and Krasil'nikova, T. G.: Estimation of the accuracy of the atmospheric refractive index recovery from Doppler shift measurements at frequencies used in the NAVSTAR system, Phys. Atmos. Ocean, 29, 602–609, 1994.
Ware, R., Rocken, C., Solheim, F., Exner, M., Schreiner, W., Anthes, R., Feng, D., Herman, B., Gorbunov, M., Sokolovskiy, S., Hardy, K., Kuo, Y., Zou, X., Trenberth, K., Meehan, T., Melbourne, W., and Businger, S.: GPS sounding of the atmosphere from lower Earth orbit: preliminary results, B. Am. Meteorol. Soc., 77, 19–40, 1996.

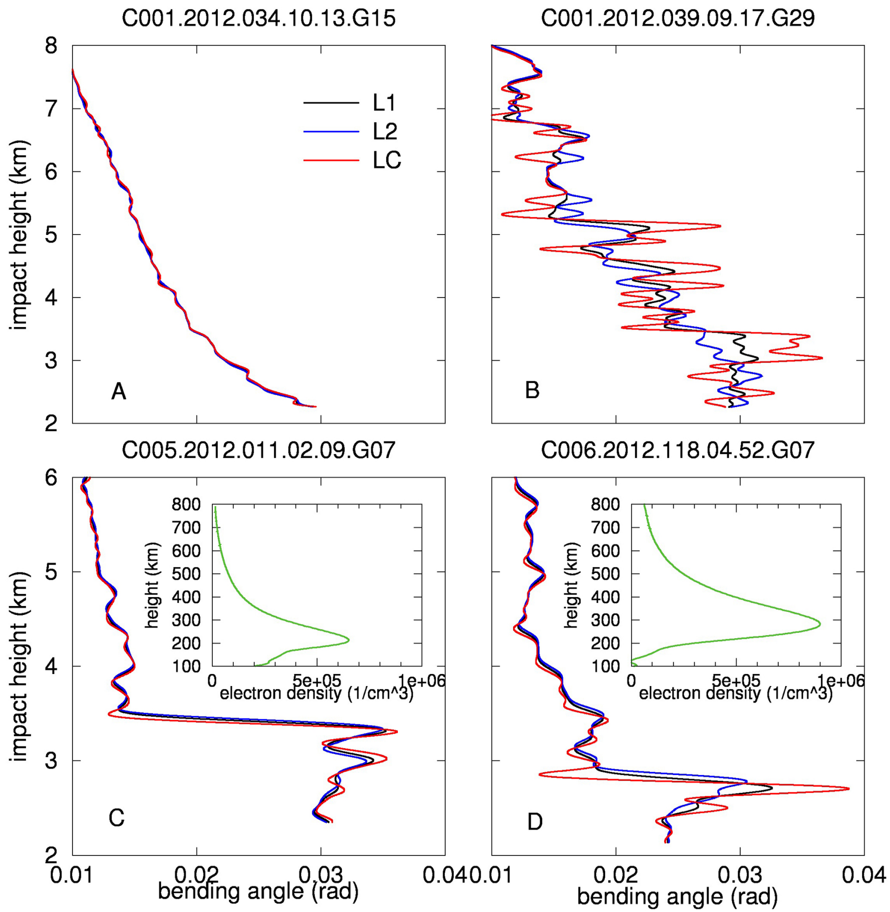

Figure 1. Examples of COSMIC L1CA (black), L2C (blue) and ionosphere-free (red) bending angles in the troposphere. (**c** and **d**) also include the ionosphere electron density profiles (green).

AMTD
8, 7781–7803, 2015

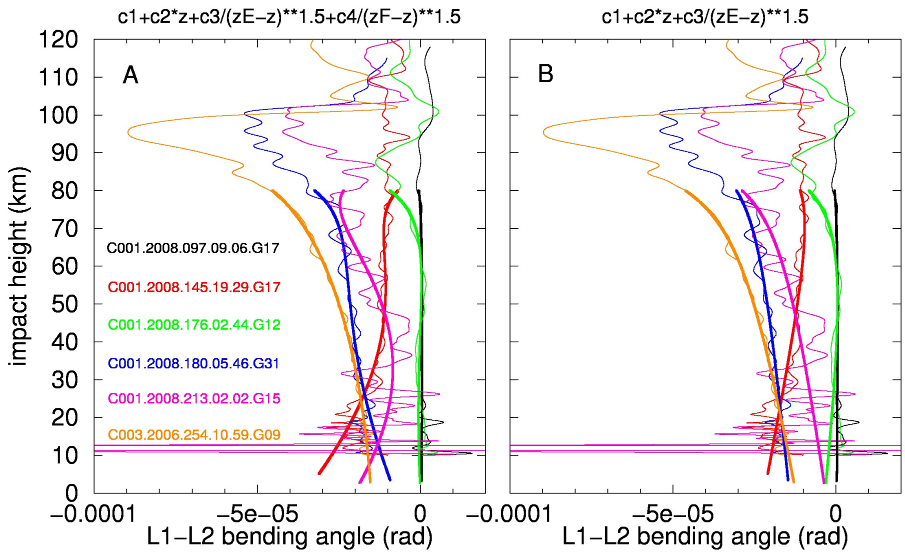

Figure 2. Examples of COSMIC L1-L2 bending angle profiles (thin lines) and fitting functions (thick lines). (**a** and **b**) correspond to different models of the fitting function.

AMTD
8, 7781–7803, 2015

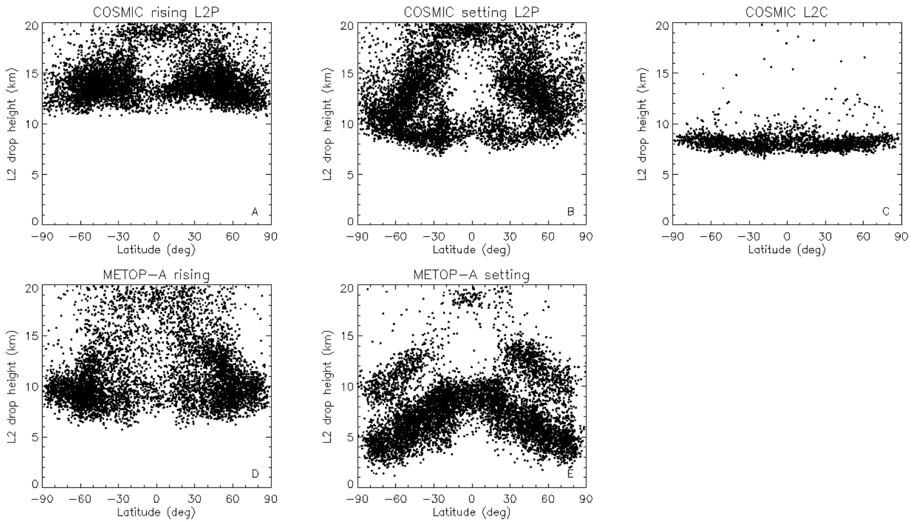

Figure 3. Latitudinal distributions of the dynamic L2 drop heights for COSMIC and METOP occultations.

AMTD
8, 7781–7803, 2015

Ionospheric correction of GPS radio occultation data in the troposphere

Z. Zeng et al.

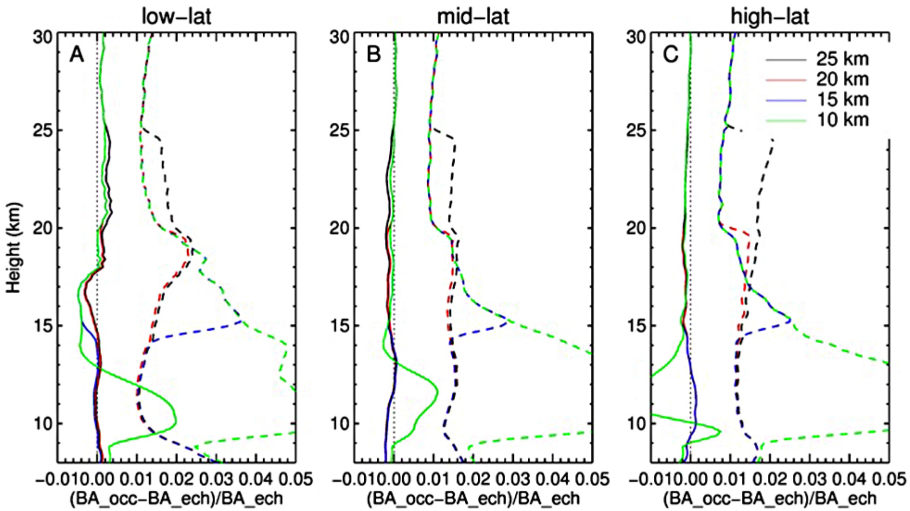

Figure 4. Mean differences (solid) and standard deviations (dashed) of retrieved COSMIC L2P bending angles for different extrapolation (transition) heights (colors indicated in **c**), relative to the co-located ECMWF bending angles over low **(a)**, mid- **(b)**, and high **(c)** latitudes.

AMTD
8, 7781–7803, 2015

Ionospheric correction of GPS radio occultation data in the troposphere

Z. Zeng et al.

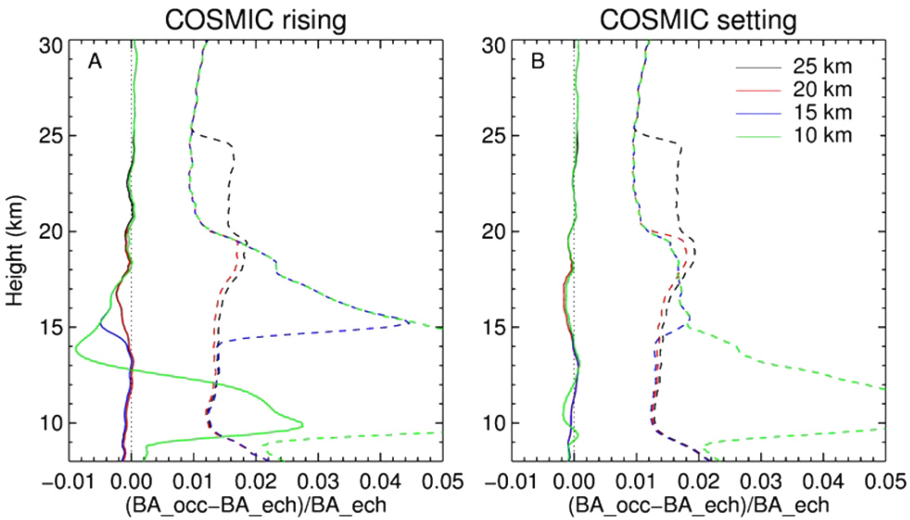

Figure 5. Similar to Fig. 4, except for the COSMIC L2P rising **(a)** and setting **(b)** occultations, for all latitudes.

AMTD
8, 7781–7803, 2015

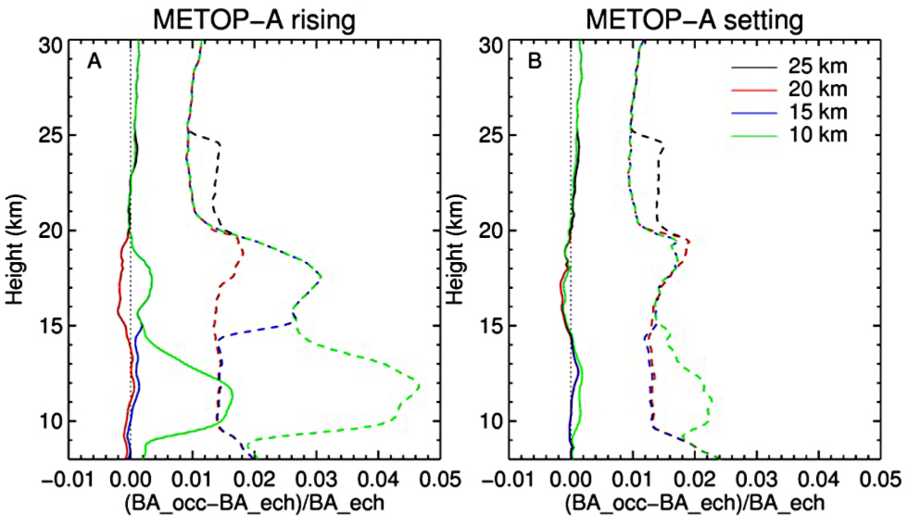

Figure 6. Similar to Fig. 4, except for the METOP rising **(a)** and setting **(b)** occultations, for all latitudes.

AMTD

8, 7781–7803, 2015

Ionospheric correction of GPS radio occultation data in the troposphere

Z. Zeng et al.

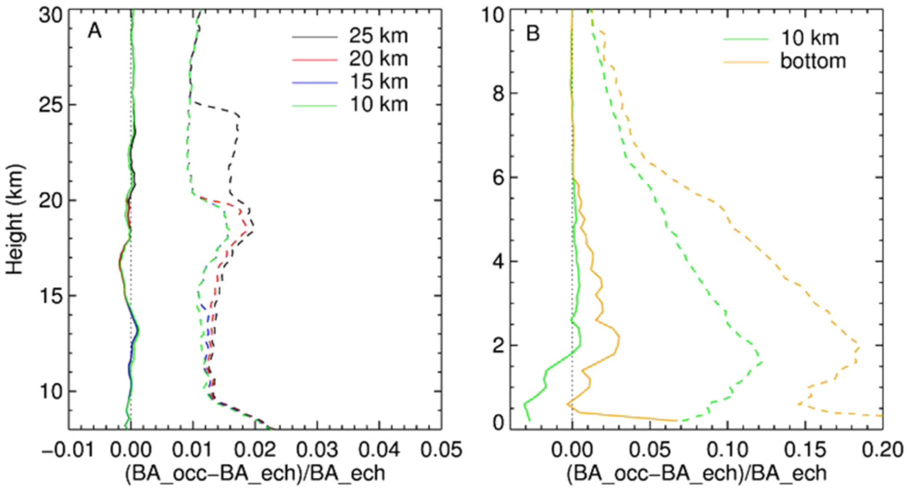

Figure 7. Similar to Fig. 4, except for the COSMIC L2C setting occultations, for all latitudes). (**a** and **b**) correspond to different height intervals and different extrapolation (transition) heights (colors indicated in panels).